Mecánica Computacional Vol. XXII
M. B. Rosales, V. H. Cortínez y D. V. Bambill (Editores)
Bahía Blanca, Argentina, Noviembre 2003

HOMOGENIZATION OF THE GENERALIZED REYNOLDS EQUATION

Gustavo C. Buscaglia*and Mohammed Jai†

*Centro Atómico Bariloche and Instituto Balseiro
San Carlos de Bariloche, Argentina
e-mail: gustavo@cab.cnea.gov.ar

†Centre de Mathématiques, INSA de Lyon, CNRS-UMR 5585
F-69621 Villeurbanne, France
e-mail: jai@insa-lyon.fr

Keywords: Lubrication, Homogenization, Magnetic storage, Roughness, Rarefaction.

Abstract. *We address the numerical modeling of roughness effects in ultra-thin gas films. Rarefaction (high Knudsen number) effects are dealt with using the Generalized Reynolds Equation, which follows from kinetic gas theory (the usual Reynolds equation is its zero-Knudsen-number limit). A homogenization procedure is proposed to rigorously account for arbitrary roughness shapes. The homogenized coefficients are obtained by the two-scale expansion methodology. The presentation is focused on head-disk magnetic storage devices, but the techniques proposed are general. Rigorous convergence proofs are available, though only for small values of the Knudsen number. Extension of the theory to arbitrary Knudsen number is under way.*

We discuss some details of the finite element implementation, in particular the use of Taylor expansions to reduce the amount of local problems to be solved, and a consistent way of calculating Newton updates.

The numerical tests concentrate on the moving-roughness case, and compare results obtained by direct calculation of rough-disk/rough-head interaction, to those obtained from the homogenized equation. Different transient effects are identified, which are properly modeled by the homogenized equation.

1. INTRODUCTION

Hard-disk interfaces are magnetic storage devices consisting of a flying head above a rigid rotating disk.[1] The need to improve the data transfer rate has led to surface-to-surface distances (air-gap thicknesses) of 30 Angstrom or less. The Boltzmann flow-modified Reynolds equation is the model of choice for the mathematical-numerical treatment of this physical problem. Accurate modeling must account for roughness effects because of machining imperfections and of fabricated irregularities that are used to avoid head-disk stiction.

When both the head and the disk surfaces are rough, their relative motion leads to an air-gap thickness that varies rapidly in space and time. If h_ϵ^H and h_ϵ^D are the elevations of, respectively, the head and the disk surfaces from a reference plane, with ϵ the roughness period (assumed unique for simplicity), we have that the air-gap thickness satisfies

$$h_{\epsilon'}(\boldsymbol{x}', t') = h_{\epsilon'}^H(\boldsymbol{x}', t') - h_{\epsilon'}^D(\boldsymbol{x}', t') \tag{1}$$

Leaving aside dynamic effects leading to motions of the head, which can easily be incorporated, we have

$$h_{\epsilon'}(\boldsymbol{x}', t') = h_0^H(\boldsymbol{x}') + \tilde{h}^H(\frac{\boldsymbol{x}'}{\epsilon'}) - h_0^D(\boldsymbol{x}') - \tilde{h}^D(\frac{\boldsymbol{x}' - t'\boldsymbol{U}}{\epsilon'}) \tag{2}$$

where functions with subscript 0 refer to the slow variations of the gap thickness, while $\tilde{h}^H$ and $\tilde{h}^D$ are *periodic* roughness functions of period one. We denote $h_0^H(\boldsymbol{x}') - h_0^D(\boldsymbol{x}')$ by $h_0(\boldsymbol{x}')$. The movement of the disk is accounted for by the shift $-t'\boldsymbol{U}$, where $\boldsymbol{U}$ is the disk speed.

The Boltzmann flow-modified Reynolds equation reads (upon normalization, in particular $\boldsymbol{x} = \boldsymbol{x}'/\ell$, $t = t'\,|\boldsymbol{U}|/\ell$, $\epsilon = \epsilon'/\ell$ and $H = h/h_{min}$)

$$\alpha\frac{\partial(PH)}{\partial t} - \nabla\cdot\left[\left(H^3P + 6KH^2\right)\nabla P\right] = -\boldsymbol{\Lambda}\cdot\nabla\left(HP\right) \tag{3}$$

with boundary condition $P(\boldsymbol{x}) = 1$ for $\boldsymbol{x} \in \partial\Omega$, where Ω is the normalized domain. The vector Λ, which is a bearing number, is assumed uniform; α is a coefficient, P is the local pressure normalized with the atmospheric pressure and K is the Knudsen number. The equation is valid up to $K = 0{,}1$. Well-posedness of this problem was proved by Chipot and Luskin.[2] For the full time-dependent case, existence and uniqueness was proved by Jai.[3]

Remark: For higher values of K the factor $H^3P + 6KH^2$ (due to Burgdorfer[4]) in (3) must be replaced by $6KH^2Q_p(HP/K)$, with Q_p the Poiseuille flow factor. We concentrate here on Burdorfer's model, but the concepts can be extended to the generalized model.

Due to Eq. (2), the coefficients in Eq. (3) vary in both space and time with scale ϵ. The computing cost of resolving these scales can be large. The number of spatial nodes in 2D grows as ϵ^{-2} and the number of required time steps as ϵ^{-1}. The global cost grows

at least as ϵ^{-3}. Simulation strategies thus require some averaging technique to remove the small scale ϵ from the problem, such as those proposed by Mitsuya et al.[5] They consist of replacing H in Eq. (3) by arithmetic or harmonic averages depending on the orientation of the roughness with respect to the flow. Averaging techniques, which date back to the work of Elrod,[6] are however heuristic counterparts to a rigorous approach referred to in the mathematical literature as *homogenization*.[7] Jai deduced the homogenization procedure for Eq. (3) in the steady case.[8] The homogenization of the time-dependent problem is a recent result of Buscaglia et al,[9] and the purpose of this article is to present those techniques in a more engineering-oriented way, to discuss their implementation, and to validate them against quasi-exact solutions obtained on very fine computational meshes.

Rigorous homogenization is most interesting for general roughness functions. When the roughness is either longitudinal or transverse the usual averaging techniques perform well. Our tests thus concern obliquely striated surfaces. Homogenization procedures in non-linear problems require multiple solutions of *local problems*, which are partial differential equation problems defined on some unit cell, representative of the roughness scale ϵ. Techniques for alleviating the computational cost of this process were proposed by Buscaglia and Jai[10] and will also be exploited here.

2. HOMOGENIZATION OF THE TRANSIENT REYNOLDS EQUATION

2.1. Two-scale analysis

We present here the formal calculations that lead to the homogenized problem to be solved, though rigorous proofs are available.[9] We follow a two-scale approach.[7] Introducing the rapid variables $\boldsymbol{y} = \frac{\boldsymbol{x}}{\epsilon}$ and $\tau = \frac{t}{\epsilon}$, we observe that

$$H(\boldsymbol{x}, t, \boldsymbol{y}, \tau) = H_0(\boldsymbol{x}, t) + \tilde{H}^H(\boldsymbol{y}) - \tilde{H}^D(\boldsymbol{y} - \tau \boldsymbol{e}_U) \tag{4}$$

where $\boldsymbol{e}_U$ is the unit vector in the direction of $\boldsymbol{U}$. In the case of a fixed attitude of the head H_0 is independent of t. We concentrate on this case later. The mathematical results will however not be restricted to H_0 independent of t since if the dynamics of the head is considered that dependence appears. The next step is to perform the following replacements in Eq. (3):

$$\frac{\partial}{\partial t} \quad \longleftarrow \quad \frac{\partial}{\partial t} + \frac{1}{\epsilon}\frac{\partial}{\partial \tau} \tag{5}$$

$$\nabla_x \quad \longleftarrow \quad \nabla_x + \frac{1}{\epsilon}\nabla_y \tag{6}$$

$$P(\boldsymbol{x}, t, \boldsymbol{y}, \tau) \quad \longleftarrow \quad P_0(\boldsymbol{x}, t, \boldsymbol{y}, \tau) + \epsilon P_1(\boldsymbol{x}, t, \boldsymbol{y}, \tau) + \epsilon^2 P_2(\boldsymbol{x}, t, \boldsymbol{y}, \tau) + ... \tag{7}$$

and then to identify the terms on the left- and right-hand sides of (3) that multiply the same power of ϵ. This leads, for each ϵ^n, to:

$\underline{n = -2}$:

$$-\nabla_y \cdot \left[\left(H^3 P_0 + 6KH^2 \right) \nabla_y P_0 \right] = 0$$

implying that P_0 *is independent of* $\boldsymbol{y}$.

$\underline{n=-1}$:

$$\alpha\frac{\partial(P_0H)}{\partial\tau}-\nabla_y\cdot\left[\left(H^3P_0+6KH^2\right)\nabla_xP_0\right]-\nabla_y\cdot\left[\left(H^3P_0+6KH^2\right)\nabla_yP_1\right]=-\boldsymbol{\Lambda}P_0\cdot\nabla_yH \tag{8}$$

Averaging this equation with respect to $\boldsymbol{y}$ and using the periodicity with respect to this variable we obtain $\alpha\frac{\partial(P_0\overline{H})}{\partial\tau}=0$ where $\overline{H}=\int_Y H(\boldsymbol{y})d\boldsymbol{y}/|Y|$ and $|Y|$ is the surface of the unit cell Y. But, from (4),

$$\overline{H}=H_0+\frac{\int_Y[\tilde{H}^H(\boldsymbol{y})-\tilde{H}^D(\boldsymbol{y}-\tau\boldsymbol{e}_U)]d\boldsymbol{y}}{|Y|}=H_0+\frac{\int_Y\tilde{H}^H(\boldsymbol{y})d\boldsymbol{y}}{|Y|}-\frac{\int_Y\tilde{H}^D(\boldsymbol{y})d\boldsymbol{y}}{|Y|}$$

so that $\overline{H}$ does not depend on τ (the surface-to-surface volume is independent of the relative position of the head and disk roughnesses), implying that P_0 *is independent of* τ.

Using now, from (4), that $\frac{\partial H}{\partial\tau}=\boldsymbol{e}_U\cdot\nabla_y\tilde{H}^D$ the problem to find P_1 for each $(\boldsymbol{x},t)$ reads

$$\begin{aligned}-\nabla_y\cdot\left[\left(H^3P_0+6KH^2\right)\nabla_yP_1\right] &= \nabla_y\cdot\left[\left(H^3P_0+6KH^2\right)\nabla_xP_0\right]\\ &\quad -\boldsymbol{\Lambda}P_0\cdot\nabla_y\left(H+\frac{\alpha}{\Lambda}\tilde{H}^D\right)\end{aligned} \tag{9}$$

where $\Lambda=|\boldsymbol{\Lambda}|$, so that $\boldsymbol{e}_U=\frac{\boldsymbol{\Lambda}}{\Lambda}$. This problem depends on $(\boldsymbol{x},t)$ through P_0, H_0 and ∇_xP_0.

$\underline{n=0}$: The equation for $n=0$, after averaging with respect to $\boldsymbol{y}$ and τ (we denote this double average by a double overline), reads

$$\alpha\frac{\partial(P_0\overline{H})}{\partial t}-\nabla_x\cdot\left[\overline{\overline{\left(H^3P_0+6KH^2\right)}\nabla_xP_0}\right]-\nabla_x\cdot\left[\overline{\overline{\left(H^3P_0+6KH^2\right)\nabla_yP_1}}\right]=-\boldsymbol{\Lambda}\cdot\nabla_x\left(P_0\overline{H}\right) \tag{10}$$

This is the so-called "homogenized problem", which, coupled to (9), allows us to determine P_0 and P_1. Since the series (7) converges, one finds a rigorous approximation of P. The coupling between (10) and (9) is very strong. In principle one should solve (9) for each and every value of $(\boldsymbol{x},t)$ and iterate going back to (10) with the new value of $\overline{\overline{\left(H^3P_0+6KH^2\right)}}$ until convergence. Some decoupling is however possible, as explained in the next paragraph.

2.2. Homogenized coefficients

Let us define the following *local problems*, to be solved in the domain Y (the unit cell of the roughness):

Local problems: For $H_0(\boldsymbol{x},t)$, $P_0(\boldsymbol{x},t)$ and τ given, find ω_1, ω_2, χ_1, χ_2, which are the only Y-periodic solutions of (with $i=1,2$)

$$-\nabla_y\cdot[\mathcal{A}(\boldsymbol{y})\nabla_y\omega_i] = \nabla_y\cdot[\mathcal{A}(\boldsymbol{y})\quad\boldsymbol{e}_i] \tag{11}$$

$$-\nabla_y\cdot[\mathcal{A}(\boldsymbol{y})\nabla_y\chi_i] = -\frac{\partial}{\partial y_i}\left[\tilde{H}^H(\boldsymbol{y})-\left(1-\frac{\alpha}{\Lambda}\right)\tilde{H}^D(\boldsymbol{y}-\tau)\right] \tag{12}$$

where

$$\begin{aligned}\mathcal{A}(\boldsymbol{y}) \;&:=\; \left(H_0(\boldsymbol{x},t)+\tilde{H}^H(\boldsymbol{y})-\tilde{H}^D(\boldsymbol{y}-\tau)\right)^3 P_0(\boldsymbol{x},t)\\ &\quad +6K\left(H_0(\boldsymbol{x},t)+\tilde{H}^H(\boldsymbol{y})-\tilde{H}^D(\boldsymbol{y}-\tau)\right)^2 \end{aligned} \tag{13}$$

These problems are small in size, since only one period of the roughness needs to be modeled. Once ω_1, ω_2, χ_1 and χ_2 are obtained, we define the *homogenized coefficients* as follows

$$\underline{\underline{\mathcal{A}}}^*(H_0(\boldsymbol{x},t),P_0(\boldsymbol{x},t)) = \begin{pmatrix} \overline{\overline{\mathcal{A}(\boldsymbol{y})\left(1+\frac{\partial\omega_1}{\partial y_1}\right)}} & \overline{\overline{\mathcal{A}(\boldsymbol{y})\frac{\partial\omega_2}{\partial y_1}}} \\ \overline{\overline{\mathcal{A}(\boldsymbol{y})\frac{\partial\omega_1}{\partial y_2}}} & \overline{\overline{\mathcal{A}(\boldsymbol{y})\left(1+\frac{\partial\omega_2}{\partial y_2}\right)}} \end{pmatrix} \tag{14}$$

$$\boldsymbol{\Theta}_1^*(H_0(\boldsymbol{x},t),P_0(\boldsymbol{x},t)) = \begin{pmatrix} \overline{H}-\overline{\overline{\mathcal{A}(\boldsymbol{y})\frac{\partial\chi_1}{\partial y_1}}} \\ -\overline{\overline{\mathcal{A}(\boldsymbol{y})\frac{\partial\chi_1}{\partial y_2}}} \end{pmatrix},\; \boldsymbol{\Theta}_2^*(H_0(\boldsymbol{x},t),P_0(\boldsymbol{x},t)) = \begin{pmatrix} -\overline{\overline{\mathcal{A}(\boldsymbol{y})\frac{\partial\chi_2}{\partial y_1}}} \\ \overline{H}-\overline{\overline{\mathcal{A}(\boldsymbol{y})\frac{\partial\chi_2}{\partial y_2}}} \end{pmatrix} \tag{15}$$

The averages with respect to $\boldsymbol{y}$ in (14)-(15) are easily performed numerically at the time of solving (11)-(12). In this way one obtains Y-averaged coefficients *for each* τ. One then averages with respect to τ by simply solving (11)-(12) for several equispaced values of τ between 0 and 1 and averaging the resulting coefficients. It should be clear from the definition of the local problems that, since (14)-(15) are averaged with respect to $\boldsymbol{y}$ and τ, the coefficients $\underline{\underline{\mathcal{A}}}^*$, $\boldsymbol{\Theta}_1^*$ and $\boldsymbol{\Theta}_2^*$ are functions of two parameters (i.e., two real numbers): $H_0(\boldsymbol{x},t)$ and $P_0(\boldsymbol{x},t)$. The dependence on these parameters is quite implicit, since it involves the solution of partial differential equations on the unit cell. It is however possible to apply the Taylor expansion technique of Buscaglia and Jai, so that only a few local problems are solved.

In what follows we will consider the functions $\underline{\underline{\mathcal{A}}}^*$, $\boldsymbol{\Theta}_1^*$ and $\boldsymbol{\Theta}_2^*$ as given. In fact, our technique consists of *building Taylor expansions* of these functions (up to order 4) by solving local problems on the unit cell Y prior to facing the global problem (Eq. 16 below) on the domain Ω. For details we refer the reader to Buscaglia and Jai.[10]

We end this section calling the reader's attention to the right-hand side of (12). In most transient cases the coefficient α takes the value 2Λ, while in the steady case (flow between two surfaces which have zero relative velocity) α is zero. The right-hand side of (12) thus changes from $\tilde{H}^H(\boldsymbol{y})+\tilde{H}^D(\boldsymbol{y}-\tau)$ in the former case, to $\tilde{H}^H(\boldsymbol{y})-\tilde{H}^D(\boldsymbol{y}-\tau)$ in the latter. While the difference between $\tilde{H}^H$ and $\tilde{H}^D$ has the physical interpretation of a distance, the sum $\tilde{H}^H+\tilde{H}^D$ that appears in the moving-roughness case is not physically intuitive. It is essential, though, for the homogenized problem to be the correct limit as ϵ tends to zero.

2.3. Homogenized equation and numerical details

It is easy to see, from (9) and (11)-(12), that

$$P_1 = \frac{\partial P_0}{\partial x_1}\,\omega_1 + \frac{\partial P_0}{\partial x_2}\,\omega_2 + P_0\Lambda_1\chi_1 + P_0\Lambda_2\chi_2 + C(\boldsymbol{x}, t, \tau)$$

where C is an arbitrary function that acts as integration constant. Replacing this into (10) and using the definitions of the homogenized coefficients one arrives at the *homogenized equation*

$$\alpha\frac{\partial(P_0\overline{H})}{\partial t} - \nabla_x\cdot\left[\underline{\underline{\mathcal{A}}}^*(H_0,P_0)\,\nabla_x P_0\right] = -\nabla_x\left[P_0\left(\Lambda_1\boldsymbol{\Theta}_1^*(H_0,P_0) + \Lambda_2\boldsymbol{\Theta}_2^*(H_0,P_0)\right)\right] \quad (16)$$

to be solved for P_0 in Ω with boundary condition $P_0 = 1$ over the boundary $\partial\Omega$. This is a transient nonlinear convection-diffusion equation, quite similar to the Reynolds equation, which is readily solved by numerical methods such as finite elements, finite differences, etc. Any solver of the Reynolds equation is easily adapted to deal with Eq. 16, while the Taylor expansions of $\underline{\underline{\mathcal{A}}}^*$, $\boldsymbol{\Theta}_1^*$ and $\boldsymbol{\Theta}_2^*$ are built in a pre-processing step, so that at runtime the calculation of the homogenized coefficients require just the evaluation of a polynomial.

In our implementation we used a Galerkin finite element method with a Crank-Nicolson treatment of the time dependence. We thus arrive at a nonlinear system of equations for each time level that is dealt with using Newton-Raphson iterations. We will skip the details here, since they are a straightforward extension to the transient case of the methodology described in a previous article.[11]

3. A TEST EXAMPLE: OBLIQUE ROUGHNESS

We consider the roughness function $f(s) = \tanh\left(5\cos(2\,\pi\,s)\right) + 1$. We assume, for the head, the roughness

$$\tilde{H}^H(x_1,x_2) = a_H f\left(\frac{x_1 - x_2}{\epsilon}\right)$$

which is inclined by 45 degrees with respect to the x_1 axis, which is the direction of motion (i.e.,$U_2 = 0$), and varies between 0 and $2a_H$. The roughness of the disk will be discussed later. As for $H_0(\boldsymbol{x})$ we have considered a Winchester-type taper-flat slider. Its geometry is presented in Fig. 1. The adopted data are as follows: ℓ = 5,540 mm, b = 0,554 mm, $h_{\text{mín}}$ = 0,15 microns,l_r = 1,01 mm, h_r = 10 microns, $h_c = -0{,}1$ microns. The slider is assumed static, so that H_0 is independent of time. We also assume $\alpha = 2$, $K = 0{,}05$ and $\Lambda = 5000$, and the initial condition is $P = 1$ throughout the domain.

Let us start with a non-moving-roughness case, to allow for comparison. For this purpose, we just set $\tilde{H}^D = 0$. We set $a_H = 1$, so that the amplitude of the roughness equals the minimum gap thickness $h_{\text{mín}}$. One may wonder whether with such a large amplitude the Reynolds equation remains valid. To answer this, one needs to evaluate the amplitude-to-wavelength ratio. Since we assume $a_H = h_{\text{mín}} = 0{,}15$ microns, for the Reynolds equation

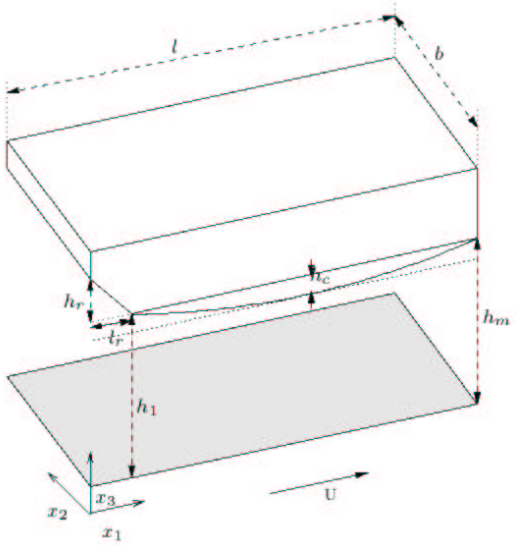

Figura 1: Sketch of the adopted geometry. The classical Winchester slider.

to be valid one must have a roughness wavelength significantly greater than the amplitude, greater than 1 micron for example. This implies that, if the number of roughness periods along the head surface is smaller than 5540, as we will assume hereafter, the Reynolds equation is indeed valid. Fabricated roughnesses reported by Mitsuya et al,[5] to consider one specific case, had a length of 40 microns, giving about 140 periods along a Winchester slider.

In a previous article we have shown that oblique roughnesses produce non-symmetric solutions. In Fig. 2 (a) we show the steady pressure field obtained after 2.5 time units with 80×8 periods. The vertical coordinate has been expanded for visualization purposes. The lack of symmetry is evident, with the upper half at significantly higher pressure than the lower half. In Fig. 2 (b) we show the homogenized pressure field P_0 obtained with the method proposed here. The homogenization procedure correctly captures the loss of vertical symmetry that appears in the exact case. Let us define the load capacity and the roll moment,

$$W(t) = \int_\Omega (P(\boldsymbol{x},t) - 1)\; d\boldsymbol{x} \qquad , \qquad \mathcal{M} = \int_\Omega P(\boldsymbol{x},t) \left(x_2 - \frac{1}{2}\frac{b}{\ell} \right)\; d\boldsymbol{x} \tag{17}$$

In Fig. 3 we compare W and M as functions of time, as calculated from the exact equation 3 with 80×8 periods and from the homogenized equation (16). Good agreement is found between the two, with some discrepancies in the initial behavior. We observe a rapid increase in W at $t = 0$, within a time of order ϵ, which is not predicted by the homogenized solution. This "pressure build-up" must thus be a consequence of the finite number of periods and disappear as ϵ tends to zero. In the same figure the roll moment predicted

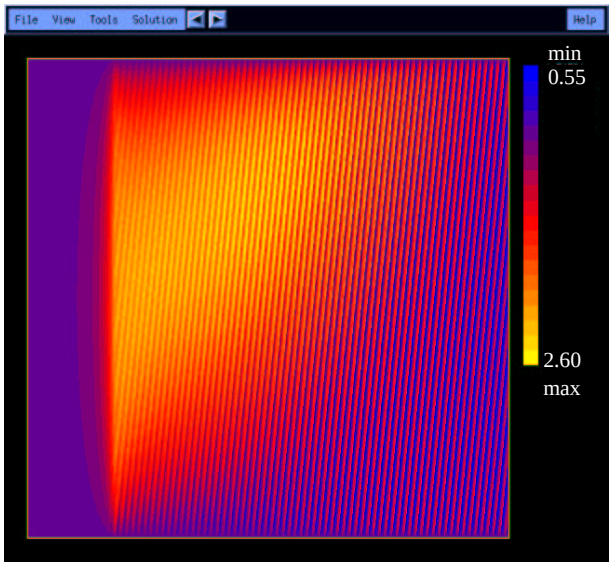

(a) 80x8 periods, t = 2.5

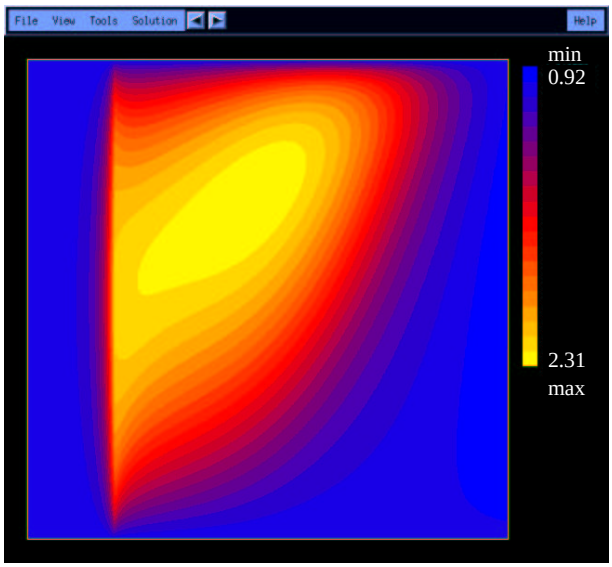

(b) Homogenized, t = 2.5

Figura 2: (a) Pressure field obtained at $t = 2{,}5$ with the exact formulation using 80×8 periods in the smooth-disk case. (b) Homogenized solution for the same case.

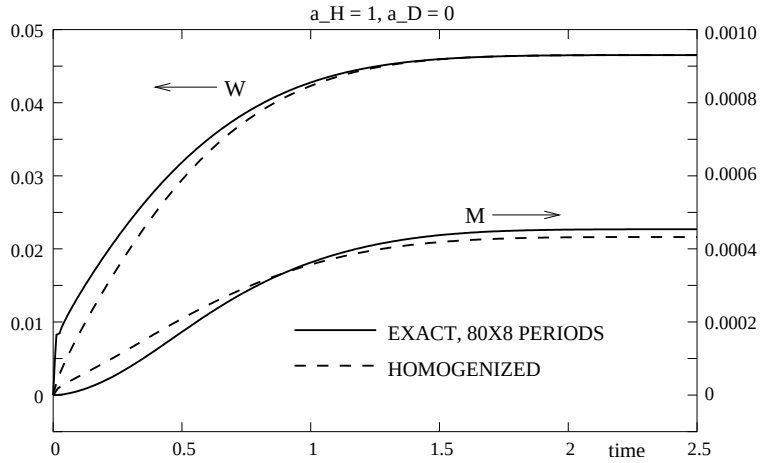

Figura 3: Load capacity $W(t)$ and roll moment $M(t)$ in the smooth-disk case. Shown are the results of the exact formulation for 80×8 periods and those of the homogenized formulation. The left vertical axis corresponds to W and the right one to M.

by the homogenization procedure can be compared to the actual roll moment produced with 80 periods. A monotonously-increasing behavior is observed, and both curves tend to approximately the same value in about the same time. Again, at $t = 0$ the behavior is different, which is attributed again to the finite number of periods. Remember that this is a non-moving-roughness case shown here just to allow for comparison.

Let us now turn to the moving-roughness case (rough-disk case). For the moving surface we consider two roughness functions, the parallel one,

$$\tilde{H}^D_{\parallel}(x_1, x_2, t) = -a_D f\left(\frac{x_1 - x_2 - t}{\epsilon}\right)$$

and the perpendicular one

$$\tilde{H}^D_{\perp}(x_1, x_2, t) = -a_D f\left(\frac{x_1 + x_2 - t}{\epsilon}\right)$$

In the following we will investigate the effects of the disk's roughness on the pressure field, on the load capacity and on the roll moment. Our objective is not to characterize these effects thoroughly, but to see whether our homogenization procedure captures them. For this purpose, we will present numerical results of the exact case with 40 and 80 periods in the x_1-direction and 4 and 8 in the x_2-direction. The adopted meshes consist of 800×80 and 1600×160 bilinear quadrilateral elements, and the time step is set to $\frac{1}{800}$ and $\frac{1}{1600}$, respectively. Moreover, a 4th-order Gaussian quadrature rule is adopted. The computational cost of these exact solutions is huge (about a month of CPU time in a Pentium-4 at 1.4 GHz). The homogenized problem, on the other hand, is solved on a mesh of 400×40 elements, using a time step of $\frac{1}{100}$. The complexity is thus at least a

factor of 256 smaller than that of the exact problem with 80×8 periods, and the CPU time is reduced to a couple of hours.

3.1. Parallel oblique roughness

This case is quite interesting because $H(\boldsymbol{x}, t)$ exhibits very strong variations with time. Consider $a_H = a_D = a$: For $t = (n + \frac{1}{2})\epsilon$, with n an arbitrary integer, the oscillatory parts of the two roughnesses cancel out ($\tilde{H}^H - \tilde{H}^D = 2a$), so that $H(\boldsymbol{x}, t) = H_0(\boldsymbol{x}) + 2a$, which is smooth. However, for $t = n\epsilon$, the roughnesses are in opposite phases and thus $H(\boldsymbol{x}, t) = H_0(\boldsymbol{x}) + 2a\, f\left((x_1 - x_2)/\epsilon\right)$ which varies between $H_0(\boldsymbol{x})$ and $H_0(\boldsymbol{x}) + 4a$ with period ϵ. This makes $W(t)$ to oscillate, also with period ϵ.

In Fig. 4(a) we plot W vs. time for the two runs of the exact problem, 40×4 periods ($\epsilon = \frac{1}{40}$) and 80×8 periods ($\epsilon = \frac{1}{80}$). Also shown there is $W(t)$ as obtained from the homogenized problem. The oscillations in $W(t)$ are evident, but their amplitude decreases with ϵ. The detail shown in 4(b) proves that the homogenized solution indeed predicts the correct mean value of $W(t)$ if the number of periods is high enough.

Comparing to Fig. 3, one observes a decrease in $W(t)$ when the disk is rough. The steady value of 0.46 falls to a time-average value of 0.34 (for $t > 2$. This is because increasing the roughness amplitude increases the mean head-to-disk distance keeping the minimum head-to-disk distance unchanged. The homogenized solution reproduces this reduction in $W(t)$ from the smooth-disk case with good accuracy.

A sensitive quantity for comparison is the roll moment, which is plotted in Fig. 5. The most remarkable observation is that the roll moment decreases by a factor of 50 when the roughness of the disk is parallel to that of the head and has the same amplitude. The homogenized solution correctly captures this phenomenon. Also, in Fig. 5 one observes that the roll moment has a maximum at $t \simeq 1$ and then decreases by about 10 percent in the 80×8-period case. This feature is not present in the 40×4-period case and is thus a subtle effect of the small scale. The homogenized solution captures this subtlety remarkably well. On the other hand, the steady-state value (for $t > 2$) of the roll moment of the homogenized solution is closer to the mean value of the roll moment of the exact solution for the 40×4-period case. This is not fully understood. It may be a consequence of the discretization errors, since the exact solutions are not truly exact but just good approximations.

3.2. Perpendicular oblique roughness

If the two roughnesses are in relative motion but arranged perpendicular to one another, then the head-to-disk spacing has the same shape at all times. The points with minimal thickness ($H = H_0$) are arranged in a square lattice oblique to the direction x_1. These points, however, move with time along the lines $x_2 = x_1 + (n + \frac{1}{2})\,\epsilon$, with n an integer. As a consequence, the load capacity $W(t)$ is much less oscillatory than in the parallel case, as can be seen in Fig. 6. One observes that the perpendicular roughness leads to a smaller

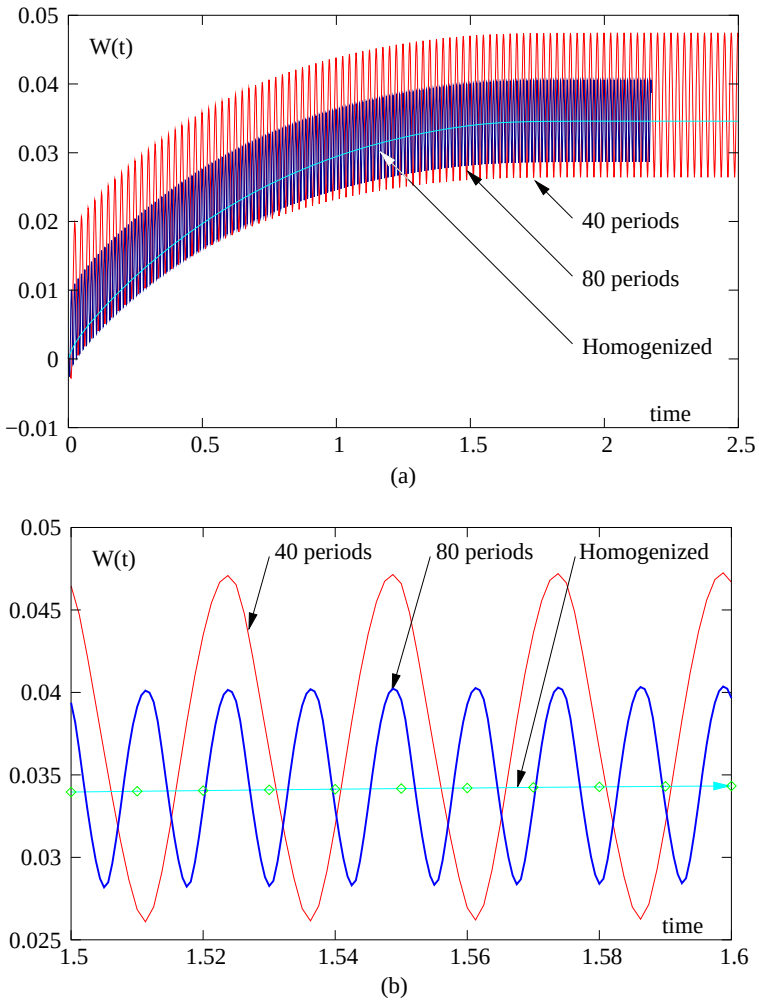

Figura 4: Time evolution of $W(t)$ for the case of parallel oblique roughness. (a) Complete evolution. (b) Detail. Compared are the exact results with 40×4 and 80×8 periods to the homogenized ones.

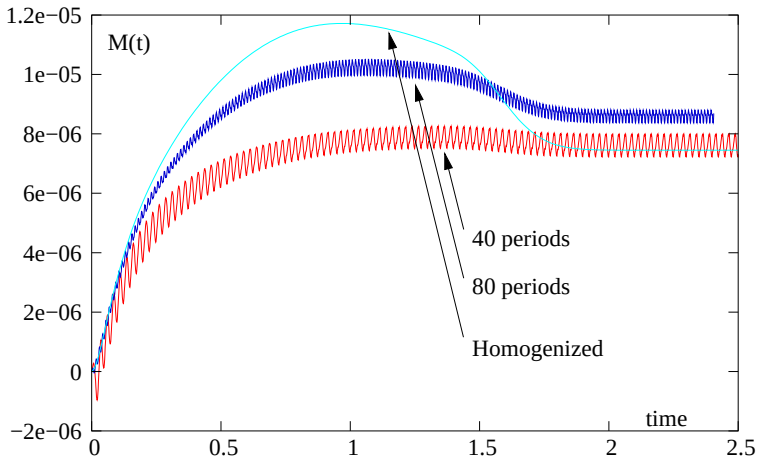

Figura 5: Time evolution of $M(t)$ for the case of parallel oblique roughness. Compared are the exact results with 40×4 and 80×8 periods to the homogenized ones.

load than the parallel one, and the homogenized solutions follow this trend.

Once again, the roll moment is another good quantity for comparison. In Fig. 7 we plot $M(t)$ in the perpendicular-roughness case, for 40 and 80 periods. M is smaller than in the smooth-disk case, by about 50 percent. This reduction is consistent with the reduction in W. All these features are correctly captured by the homogenized solution. On the other hand, the discrepancies in the initial behavior ($t < 1$) between the exact and homogenized solutions are again present here, as in the smooth-disk case.

3.3. Pressure fields

We end up this section displaying a few pressure fields. In Fig. 8 (left) we show contour plots calculated at $t = 2{,}5$ for the exact problem with 80×8 periods (a), and for the homogenized problem (b), in the case of parallel oblique roughness. The x_2 coordinate has been expanded by a factor of 10 to ease the visualization.

By direct comparison to Fig. 2 one observes that the relative motion of head and disk greatly modifies the pressure field. Moreover, the homogenized pressure field is an excellent approximation to the exact one. Analogous plots are shown in Fig. 8 (right) for the case of perpendicular oblique roughness. Comparing to the previous figure, it is clear in the exact solutions that the orientation of the disk's roughness greatly affects the pressure field. It is also clear that the homogenization procedure presented here provides a suitable approximation in all cases.

4. CONCLUSIONS

In this article we have tried to motivate the use of rigorous homogenization procedures in the analysis of lubrication problems in which roughness effects are significant.

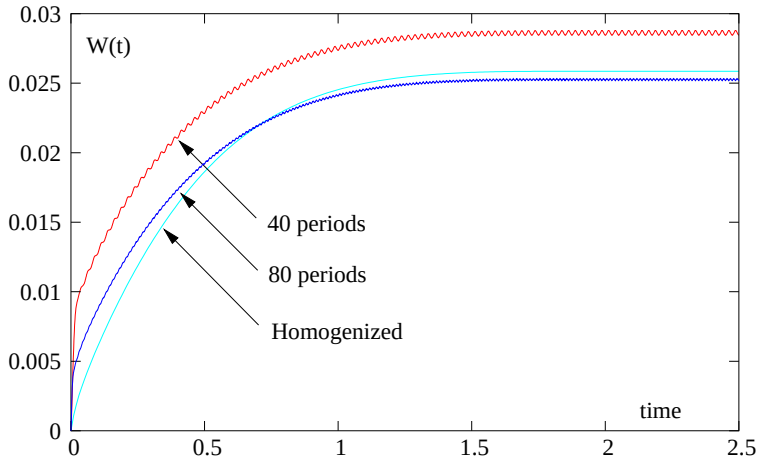

Figura 6: Time evolution of $W(t)$ for the case of perpendicular oblique roughness. Compared are the exact results with 40×4 and 80×8 periods to the homogenized ones.

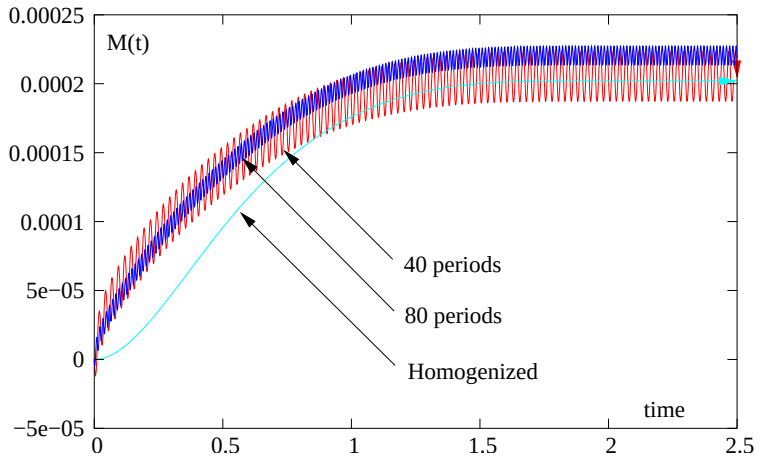

Figura 7: Time evolution of $M(t)$ for the case of perpendicular oblique roughness. Compared are the exact results with 40×4 and 80×8 periods to the homogenized ones.

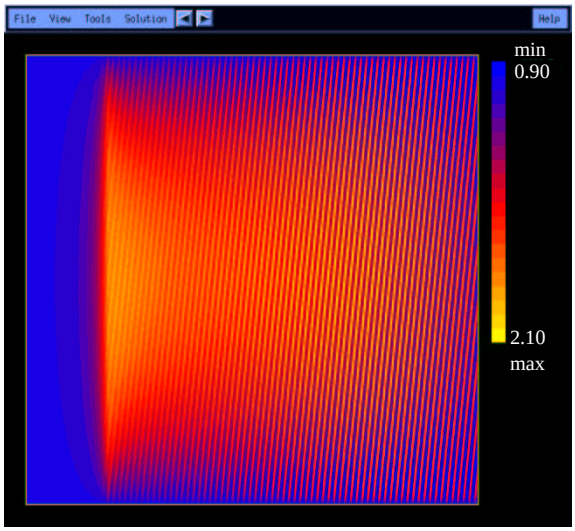

(a) 80x8 periods, t = 2.5

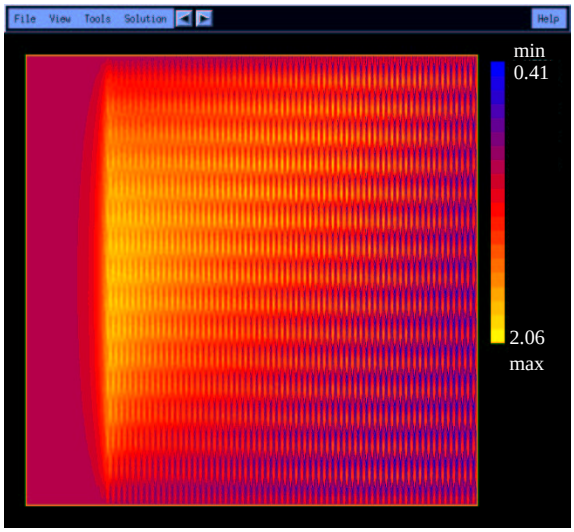

(a) 80x8 periods, t = 2.5

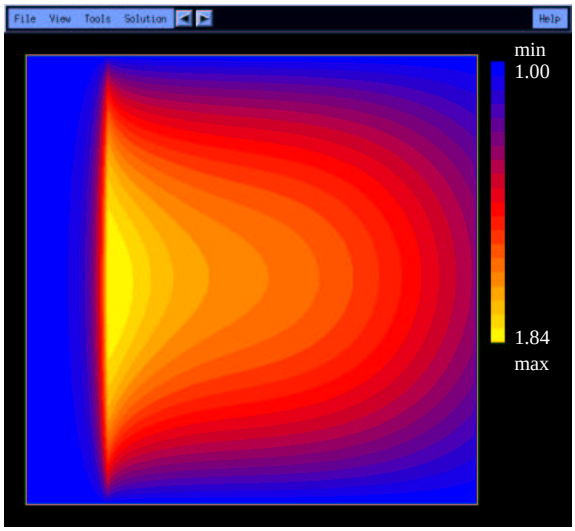

(b) Homogenized, t = 2.5

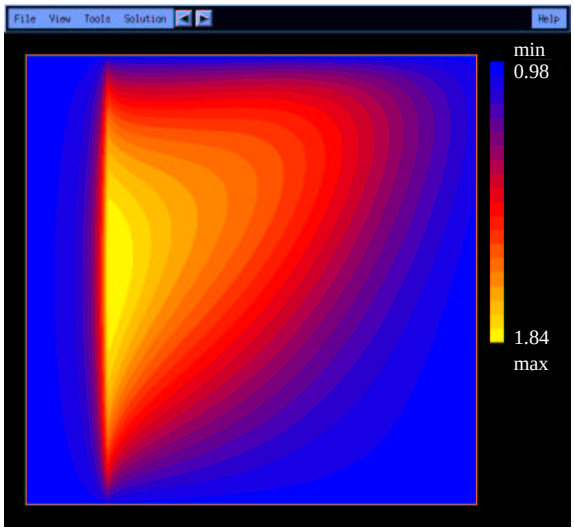

(b) Homogenized, t = 2.5

Figura 8: Contour zones of the pressure field at $t = 2{,}5$. Left: Parallel roughness case. Right: Perpendicular roughness case. (a) Exact solution with 80×8 periods. (b) Homogenized solution.

Standard averaging techniques are conceptually simpler, since they rely upon explicit analytical solutions. These analytical solutions correspond to the one-dimensional parallel and transverse roughnesses. However, the generalization of averaging techniques to arbitrary roughness shapes is not straightforward. Moreover, when the roughness shape is oblique to the flow direction significant errors may be introduced by the averaging techniques which are automatically avoided when homogenization is used.

Direct simulation of lubrication problems accounting for the precise shape of each roughness feature takes of course averaging or homogenization techniques out of the picture. For the magnetic head-disk contact problem direct simulation is nowadays affordable, though not yet inexpensive, when the disk is smooth. When both surfaces are rough their relative motion makes direct simulations much more burdensome. As a consequence, averaging and homogenization will remain necessary for some time in the analysis and design of hard-disk interfaces.

In this article, we have presented the formal derivation of a homogenization procedure for the moving-roughness compressible lubrication problem. This procedure was rigorously justified in a recent mathematical article.[9] The numerical implementation has been briefly discussed, and numerical results shown. The numerical results, which correspond to obliquely-striated surfaces for both the head and the disk, put forward significant and quite unexpected effects of special roughness shapes. They also show that the proposed homogenization procedure captures both qualitatively and quantitatively the main roughness-induced phenomena that arise in the head-disk contact problem. To the authors' knowledge, no averaging method would perform as well as the proposed homogenization method, in particular in the prediction of the roll moment on the head. It would be interesting that other groups benchmark novel averaging methods in the obliquely-striated-roughness case, which has proved to be quite challenging.

This work was partially supported by ANPCyT through grans PICT 12-6337 and 12-09848, and by a Bonus Qualité Recherche awarded by the INSA de Lyon.

REFERENCIAS

[1] B. Bushan, *"Tribology and Mechanics of Magnetic Storage Devices"*, Springer Verlag (1990).

[2] M. Chipot and M. Luskin, "Existence and uniqueness of solutions to the compressible Reynolds lubrication equation", *SIAM J. Math. Anal.* **17**, 1390–1399 (1986).

[3] M. Jai, "Existence and uniqueness of solutions of the parabolic nonlinear compressible Reynolds lubrication equation", *Nonlinear Analysis* **43**, 655–682 (2001).

[4] B. Burgdorfer, "The influence of the molecular mean free path on the performance of hydrodynamic gas lubricated bearings", *ASME J. of Basic Engineering* **81** , 99–100 (1959).

[5] Y. Mitsuya, T. Ohkubo, and H. Ota, "Averaged Reynolds equation extended to gas lubricant possessing surface roughness in the slip flow regime: Approximate method and confirmation experiments", *ASME J. of Tribology* **111**, 495–503 (1989).

[6] H. Elrod, "Thin film lubrication theory for Newtonien fluid with surfaces possessing striated roughness or grooving", *ASME J. of Tribology*, 484–489 (Oct. 1973).

[7] A. Bensoussan, J. L. Lions and G. Papanicolaou, *Asymptotic analysis for periodic structure*, North Holland (1978).

[8] M. Jai, "Homogenization and two-scale convergence of the compressible Reynolds lubrication equation modeling the flying characteristics of a rough magnetic head over a rough rigid-disk surface", *Math. Modeling and Numer. Anal.* **29**, 199–233(1995) .

[9] G. Buscaglia, I. Ciuperca and M. Jai, "Homogenization and two-scale analysis of the transient compressible Reynolds equation", *Asymptotic Analysis* **32**, 131–152 (2002).

[10] G. Buscaglia and M. Jai, "Sensitivity analysis and Taylor expansions in numerical homogenization problems", *Numer. Math.* **85**, 49–75 (2000).

[11] G. Buscaglia and M. Jai, "A new numerical scheme for non uniform homogenized problems: Application to the nonlinear Reynolds compressible equation", *Mathematical Problems in Engineering* **7**, 355–377 (2001).